Structure and Transport Anomalies in Soft Colloids

Samanvaya Srivastava, Lynden A. Archer, and Suresh Narayanan

Phys. Rev. Lett. **110**, 148302 — Published 3 April 2013

DOI: 10.1103/PhysRevLett.110.148302

Structure and Transport Anomalies in Soft Colloids

Samanvaya Srivastava and Lynden A. Archer*

School of Chemical and Biomolecular Engineering, Cornell University, Ithaca, NY 14853, USA

Suresh Narayanan

Advanced Photon Source, Argonne National Laboratory, Argonne, IL 60439, USA

Anomalous trends in nanoparticle correlation and motion are reported in soft nanoparticle suspensions using static and dynamic X–ray scattering measurements. Contrary to normal expectations, we find that particle–particle correlations decrease and particle dynamics become faster as volume fraction rises above a critical particle loading associated with overlap. Our observations bear many similarities to the cascade of structural and transport anomalies reported for complex, network forming molecular fluids such as water, and are argued to share similar physical origins.

Increasing the concentration of particles in a dilute suspension normally decreases the space available for placing new particles, which lowers the configurational entropy, increases correlations between the particle centers, and slows down particle motion. In this Letter we report the structure, rheology, and dynamics of suspensions of soft, oligomer–grafted nanoparticles dispersed in a fluid chemically identical to the attached chains. We find that the suspensions exhibit anomalous structural and dynamic properties wherein inter–particle correlations decrease and particle dynamics speed–up with an increase in the volume fraction ϕ above a critical value. Such anomalous behavior has been reported for complex liquids such as water [1,2] and silica [3] and has been long argued to exist for systems with non–directional, core–softened repulsive interactions [4–10]; herein we report the first instance of experimental observation of such behavior in a soft colloidal fluid.

Colloidal suspensions have been extensively studied as models for atomic and molecular liquids [11–14]. They share important similarities, including disordered structure, analogous long time dynamics, glass/jamming transitions, and ability to undergo solid–liquid phase transitions upon application of suitable density, pressure, or thermal fields. Recently, soft colloids have garnered significant attention for their ability to mimic more complex interactions in molecular

fluids with non–hard–sphere like interactions [4–6,15–26]. Among the most striking observations reported in these systems is an anomalous transition to a state of reduced inter–particle correlation near the jamming transition [4–6,15–19,23–26]. Suspensions of a variety of soft particles including soft microgel particles [15], tapioca pearls [16,17], concentrated star polymer solutions [18] and nano–emulsions [19] have been shown to exhibit anomalous structural characteristics. These trends are analogous to those observed in water, wherein isothermal compression allows a fifth molecule to enter into the tetrahedral network of molecules, leading to a decrease in structural order [1,2]. This reduced order manifests as anomalous, high diffusivities upon compression [1,2,27] as well as an anomalous reduction in density, but none of the other traits associated with the appearance of anomalous structure in molecular liquids have so far been observed in soft colloidal systems.

We previously reported nanoparticle suspensions, created by densely grafting oligomeric polyethylene glycol (PEG) chains (M_W ~ 450 Da) on nanometer–sized silica (SiO_2) and suspended in a PEG oligomer (M_W ~ 550 Da) [28, 29]. These materials provide a good physical model for soft particle suspensions because enthalpic forces are completely turned off and thermal forces are significant [29]. In particular, we observed that these suspensions manifest little to no aging and are able to reach an equilibrium, Newtonian fluid flow regime even at particle loadings beyond the apparent "jamming" transition where the zero shear viscosity η of the suspensions appear to diverge (see Figure 1 and [29]).

Figure 1a and 1b report the evolution of the structure factor $S(q)\left(=I(q)/\lim_{\phi\to 0} I(q)\right)$ with increasing ϕ for suspensions comprising of SiO_2 core particle with diameters d = 10 nm and 24 nm. Measurements were performed using small angle X–ray scattering (SAXS) experiments at Sector 12–ID–B of the Advanced Photon Source over extremely small exposure times (~ 100 ms). *S(q)* is the Fourier transform of the particle correlation function *g(r)* and the height of the first peak of the structure factor, S_1 is a direct experimental measure of the degree of nearest neighbor correlations among scatterers. S_1 continuously increases with ϕ for a suspension of hard spheres until the jamming transition. It is evident from Figure 1a – c that for a suspension of soft particles, S_1 exhibits a pronounced maximum at a specific, particle-diameter dependent volume fraction $\phi = \phi_S(d)$ (dashed lines in Figure 1c), indicating that particles become increasingly uncorrelated with increasing ϕ above ϕ_S.

The observed increase in S_1 for $\phi < \phi_S$ can be interpreted using conventional arguments for hard–sphere suspensions. At low to moderate loadings, particles explore the entire configurational space and minimize the overall system energy while managing to avoid energetically expensive overlaps. This produces enhanced particle–particle correlations as ϕ rises. In contrast to a system of hard sphere particles, the extra degrees of freedom associated with particle softness facilitates introduction of new particles even beyond the onset of particle–particle contact at $\phi = \phi_S$, coinciding with the upturn in η (Figure 1c). Such particle accommodation doesn't necessarily enhance correlations between the particles and, additionally, non–uniform compression of the flexible PEG oligomer corona tethered to the particle cores leads to a progressive loss of correlation among particles with increasing ϕ.

The degree of homogeneity in these suspensions can also be estimated by observing the trends in S_0 ($=\lim_{q\to 0} S(q)$), which is related to the isothermal compressibility of a suspension. The minimum q achievable with the current instrument is 0.08 nm^{-1}, and we define $S(q)$ at this value as S_m. Figure 1d shows that S_m continually decreases for $\phi < \phi_S$ and subsequently approaches a constant for $\phi \geq \phi_S$. The dashed lines in the figure are the expected trends for a suspension of hard spheres. The trends in S_m as well as S_1 for suspensions of the SiO_2–PEG nanoparticles are evidently quite different from expectations for hard sphere suspensions. Notwithstanding these differences, the inter particle separation ($d_p = 2\pi/q_{S_1}$) is found to continually decreases with increasing ϕ and coincides fairly well with the theoretical estimates for a suspension of hard spheres, $d_p = d(0.63/\phi)^{1/3}$. This result means that the anomalous reduction in particle–particle correlations beyond ϕ_S is not a result of large–scale variations in the particle arrangement, but rather are a manifestation of non–uniform particle deformation.

Insights into the dynamics processes in these suspensions can be provided by the time–correlation of the scattering intensity patterns, as probed through X–ray photon correlation spectroscopy (XPCS) measurements, which were carried out at Sector 8–ID–I of the Advanced Photon Source. Care was taken during the course of these measurements to exclude the effects of radiation damage and x–ray heating. Specifically, by varying the x-ray intensity and repeating measurements at fixed intensity over different exposure times and at different sample locations, it was possible to empirically assess the effect of radiation exposure on the studied materials. And, at the incident intensities selected for our XPCS measurements, the total scattering intensity

was found to remain essentially constant over all of these variations, indicating no appreciable changes in the system due to x–ray irradiation. Thus, the scattering intensity auto correlation can be assumed to reveal the nanoscale dynamics of the system. A contour map of the two–time intensity auto correlation function $G(q,t_1,t_2)\left(=\langle I(q,t_1)I(q,t_2)\rangle/\langle I(q,t_1)\rangle\langle I(q,t_2)\rangle\right)$ for a SiO_2–PEG nanoparticle suspensions is reported in Figure 2a and clearly indicates the absence of any time-dependent slowing down or speeding up of the nanoparticle motions [30]. These results in conjunction with the decidedly weak time variations in rheological characteristics of the suspensions [29] also nicely establish that aging plays a negligible role in dynamics of these suspensions. Further averaging G (q, t_1, t_2) for a fixed time interval, $t = t_2 - t_1$ yields the time autocorrelation of the scattering intensity patterns as $g_2(q,t)=\langle G(q,t_1,t)\rangle_{t_1}$, and subsequently the dynamic structure factor: $f(q,t) = ((g_2(q,t) - 1)/b)^{1/2}$ [31]. Here, b is an instrument–dependent Seigert factor.

Colloidal suspensions have been reported to exhibit two distinct relaxation processes near the jamming transition: a fast relaxation originating from in–cage rattling motion of particles with time scales typically < 1 ms, which is outside the measurement window for XPCS; and a slower relaxation originating from cage–escape [13,32]. The slower processes are characterized by partial correlation among scatterers at small times corresponding to $f(q,t) < 1$ and are succinctly captured at ϕ values both below and above ϕ_S, as shown in Figure 2b and 2c, respectively. While a terminal relaxation ($f(q,t) \sim 0$ at large t) with finite relaxation time scales is expected for unjammed suspensions (Figure 2b), the appearance of a terminal relaxation regime for $\phi > \phi_S$ (Figure 2c) is in stark contrast to usual observations in jammed colloidal suspensions, even comprising of soft particles [15]. It is consistent, however, with our earlier report [29] that suspensions of well-grafted, hairy nanoparticles are able to reach an equilibrium state characterized by a Newtonian flow regime and is in accord with the aforementioned non–aging rheological characteristics of SiO_2–PEG/PEG suspensions.

We conjecture that a combination of factors might be responsible for the unique "jammed"–yet–equilibrated dynamic characteristics of the SiO_2–PEG/PEG suspensions: i) the small size of the particles mean that the Brownian stresses are quite large $O(10^5$ Pa) and easily exceed the viscous loss modulus G'' of the "jammed" suspension [29], which means that there is a strong driving force for relaxation; ii) segmental motion of the tethered PEG oligomers provides an

important *internal lubrication* effect among overlapping particles, which facilitates particle relaxation and cage escape; and iii) the flexibility of the tethered PEG chains imparts softness to the particles, allowing local system rearrangements on the way to equilibrium. An advantage of these characteristics is that the time scale τ associated with the cage–escape motion of the nanoparticles is visible in the dynamic structure factor on convenient timescales for XPCS. By fitting the measured $f(q,t)$ (Figure 2b and 2c) with a compressed exponential function [31]:

$$f(q,t) = f_0 \exp\left[-\left(\frac{t}{\tau}\right)^{\beta}\right] \tag{1}$$

it is possible to determine the time scale τ and the compression exponent β. Further, the nature of the forces acting on the nanoparticles can be elucidated by the wave vector dependence of τ and is presented in Figure 3. A characteristic $1/q$ scaling is observed for nearly all the suspensions studied, indicative of slow, hyperdiffusive motion of the nanoparticles. Similar ballistic motion of scatterers has been reported in a variety of jammed soft solids as well as glassy liquids [30,31,33–37] and is thought to arise from residual stress dipoles associated with systems going through the jamming transition. However, relaxation of these stress dipoles is expected to lead to significant aging behavior, which is inconsistent with our findings. Equally significant is the fact that at low nanoparticle loadings, a transition to a diffusive scaling, $\tau \propto 1/q^2$, is found for the 24 nm particles, indicating that the hyperdiffusive behavior is in fact not directly associated with particle–particle overlap or jamming. This transition from diffusive to hyperdiffusive particle dynamics with increasing particle (scatterer) density is, to our knowledge, the first experimental report of the phenomenon.

Figure 4 reports the characteristic relaxation time τ for the suspensions as a function of ϕ for four different particle sizes. Initially, τ grows with increasing ϕ as expected and is described fairly well using a fit of the Vogel–Fulcher–Tammann (VFT) form [22,32], $\tau = \tau_\infty \exp\left[A/(\phi_0 - \phi)\right]$, shown as solid lines in the figure. But beyond a critical $\phi = \phi_D$, particle dynamics clearly speed up, leading to a non–monotonic dependence of τ on ϕ in all but the largest, $d \approx 40$ nm, particles. As pointed out earlier, such counterintuitive transport behavior has heretofore only been observed in complex liquids such as water [1,2,27]. Simulation studies for model systems interacting with Hertzian [4–6], Gaussian [5–8] or other core–softened repulsive potentials [5,6,9,10,24], with or without hydrodynamic interactions, have predicted the

underlying dynamic anomaly to occurs when $(\partial s_{ex}/\partial \ln \rho)_T > 0.42$, indicating that it should naturally follow the occurrence of a structural anomaly ($(\partial s_{ex}/\partial \ln \rho)_T > 0$) [10]. s_{ex}, ρ and T denote excess entropy, density and temperature, respectively. That this "cascade" of anomalies [2,10] is observed ($\phi_D > \phi_S$), for the first time, in our SiO_2–PEG/PEG suspensions indicates that these suspensions are good physical models for fluids in which core–softened repulsive interactions dominate. Our findings also support the hypothesis that the anomalous trends in dynamics of such fluids occur independent of hydrodynamic interactions between the particles and solvent [5,6]. The structural and transport trends eventually return to normalcy in water owing to extremely steep short range repulsion in the limit of very high density [1,2,8] and we expect the same to occur in the suspensions investigated here. Soft nanoparticle suspension compositions expected to achieve this limiting behavior are in such an extreme state of overlap that crystallization prevents characterization of their structural and dynamic properties. Decreasing particle softness (by increasing d) leads to progressively earlier onset of crystallization and prevents observation of the dynamic anomaly in the largest, 40 nm, nanoparticle suspensions studied.

In summary, we have studied suspensions of oligomer–grafted nanoparticles in an oligomeric fluid host and find structural and dynamic trends that are consistent with theory, but heretofore not observed experimentally. In particular we find that particle–particle correlations increase with ϕ only up to a critical value ϕ_S, whereafter they decrease with increasing particle loading in the suspensions. Additionally, we find that the diffusivity of the particles exhibit a similar transition wherein the particle mobility first falls with increasing ϕ, but then rises for $\phi > \phi_D$. Complex, network forming molecular fluids such as water and silica as well as systems interacting with core–softened repulsive interactions have been shown previously to exhibit a similar cascade of structural and transport anomalies. Our empirical findings lend support to an emerging consensus from simulation studies that softness of inter-particle/molecular repulsive forces allows for strong entropic gains that more than compensate for the energetic cost of molecule/particles overlaps, producing the observed cascade of anomalies. Our observations also suggest that soft nano–colloids extend the tool–box of the experimental physicist interested in using suspensions for studying interactions and dynamics in molecular liquids.

ACKNOWLEDGEMENTS

This work was supported by the National Science Foundation, Award No. DMR–1006323 and by Award No. KUS–C1–018–02, made by King Abdullah University of Science and Technology (KAUST). Use of the Advanced Photon Source, operated by Argonne National Laboratory, was supported by the U.S. DOE under Contract No. DE–AC02–06CH11357. We acknowledge Prof. A. D. Stroock for helpful discussions.

REFERENCES

*laa25@cornell.edu

[1] A. Scala *et al.*, Nature **406**, 166 (2000).

[2] J. E. Errington and P. G. Debenedetti, Nature **409**, 318 (2001).

[3] M. S. Shell, P. G. Debenedetti and A. Z. Panagiotopoulos, Phys. Rev. E **66**, 011202 (2002).

[4] L. Berthier, A. J. Moreno and G. Szamel, Phys. Rev. E **82**, 060501(R) (2010).

[5] M. J. Pond, J. E. Errington and T. M. Truskett, J. Chem. Phys. **134**, 081101 (2011).

[6] M. J. Pond, J. E. Errington and T. M. Truskett, Soft Matter **7**, 9859 (2011).

[7] A. B. de Oliveira *et al.*, J. Chem. Phys. **124**, 084505 (2006).

[8] W. P. Krekelberg *et al.*, Phys. Rev. E **79**, 031203 (2009).

[9] P. Kumar *et al.*, Phys. Rev. E **72**, 021501 (2005).

[10] J. E. Errington, T. M. Truskett and J. Mittal, J. Chem. Phys. **125**, 244502 (2006).

[11] P. N. Pusey and W. van Megen, Nature **320**, 340 (1986).

[12] P. N. Pusey and W. van Megen, Phys. Rev. Lett. **59**, 2083 (1987).

[13] E. R.Weeks *et al.*, Science **287**, 627 (2000).

[14] L. Cipelletti and E. R. Weeks, *Glassy dynamics and dynamical heterogeneity in colloids, Dynamical Heterogeneities in Glasses, Colloids, and Granular Media*, edited by L. Berthier, G. Biroli, J.–P. Bouchaud, L. Cipelletti and W. van Saarloos (Oxford University Press, 2011).

[15] Z. Zhang *et al.*, Nature **459**, 230 (2009).

[16] X. Cheng, Phys. Rev. E **81**, 031301 (2010).

[17] X. Cheng, Soft Matter **6**, 2931 (2010).

[18] G. A. McConnell and A. P. Gast, Macromolecules **30**, 435 (1997).

[19] S. Graves *et al.*, J. Chem. Phys. **122**, 134703 (2005).

[20] K. N. Pham *et al.*, Science **296**, 104 (2002).

[21] C. Mayer *et al.*, Nature Materials **7**, 780 (2008).

[22] J. Mattsson *et al.*, Nature **462**, 83 (2009).

[23] M. Watzlawek, H. Löwen, and C. N. Likos, J. Phys.: Condens. Matter **10**, 8189 (1998).

[24] G. Foffi *et al.*, Phys. Rev. Lett. **90**, 238301 (2003).

[25] L. E. Silbert, A. J. Liu and S. R. Nagel, Phys. Rev. E **73**, 041304 (2006).

[26] H. Jacquin, L. Berthier and F. Zamponi, Phys. Rev. Lett. **106**, 135702 (2011).

[27] K. R. Harris and L. A. Woolf, J. C. S. Faraday I 76, 377 (1980); K. R. Harris and P. J. Newitt, J. Chem. Eng. Data **42**, 346 (1997).

[28] J. L. Nugent, S. S. Moganty, D. A. Yanga and L.A. Archer, J. Materials Chem. **21**, 10094 (2011).

[29] S. Srivastava, J. H. Shin and L. A. Archer, Soft Matter **8**, 4097 (2012).

[30] A. Madsen *et al.*, New J. Phys. **12**, 055001 (2010).

[31] R. L. Leheny, Curr. Op. Colloid Interface Sci. **17**, 3 (2012).

[32] G. Brambilla *et al.*, Phys. Rev. Lett. **102**, 085703 (2009).

[33] L. Cipelletti *et al.*, Faraday Discuss. **123**, 237 (2003).

[34] R. Bandyopadhyay *et al.*, Phys. Rev. Lett. **93**, 228302 (2004).

[35] H. Guo *et al.*, Phys. Rev. E **75**, 041401 (2007).

[36] H. Guo *et al.*, Phys. Rev. Lett. **102**, 075702 (2009).

[37] H. Guo *et al.*, J. Chem. Phys. **135**, 154903 (2011).

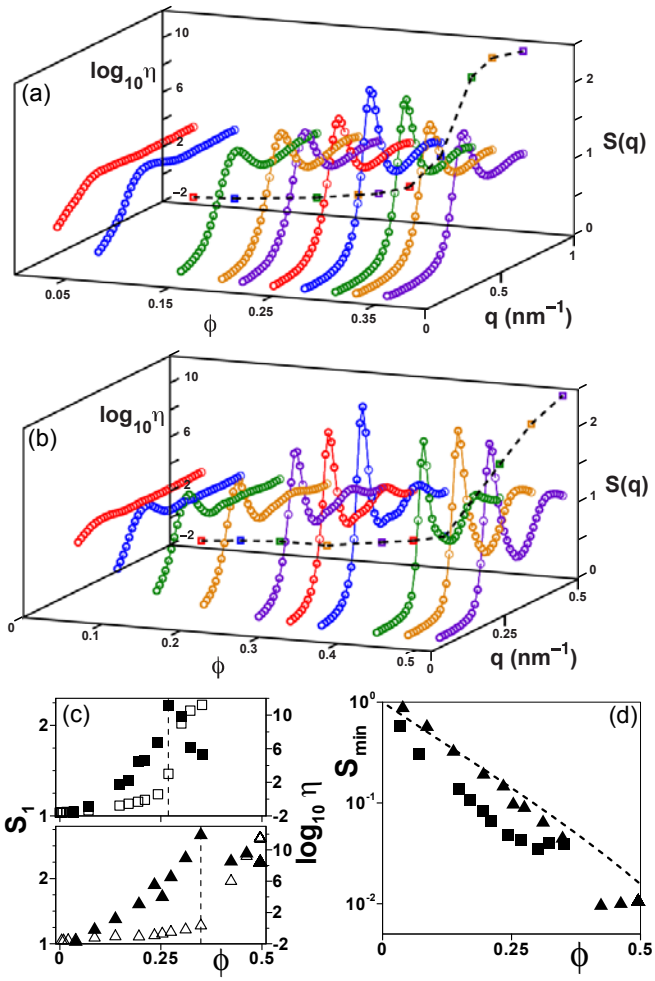

Figure 1| Structure factor evolution for soft colloids. (a), (b) Structure factor $S(q)$ and zero shear viscosity η vs. particle volume fraction ϕ, (b) the maximum in $S(q)$, S_1 and η vs. ϕ (closed and open symbols, respectively) and (d) the minimum value of $S(q)$, S_m vs. ϕ for suspensions with d = 10 nm (squares) and 24 nm (triangles) particles, respectively. In (a) and (b), η vs. ϕ is depicted on the back panels. Dashed lines are a guide to the eye in (a) and (b), denote the position of maxima in S_1 in (c) and S_m for hard sphere systems in (d).

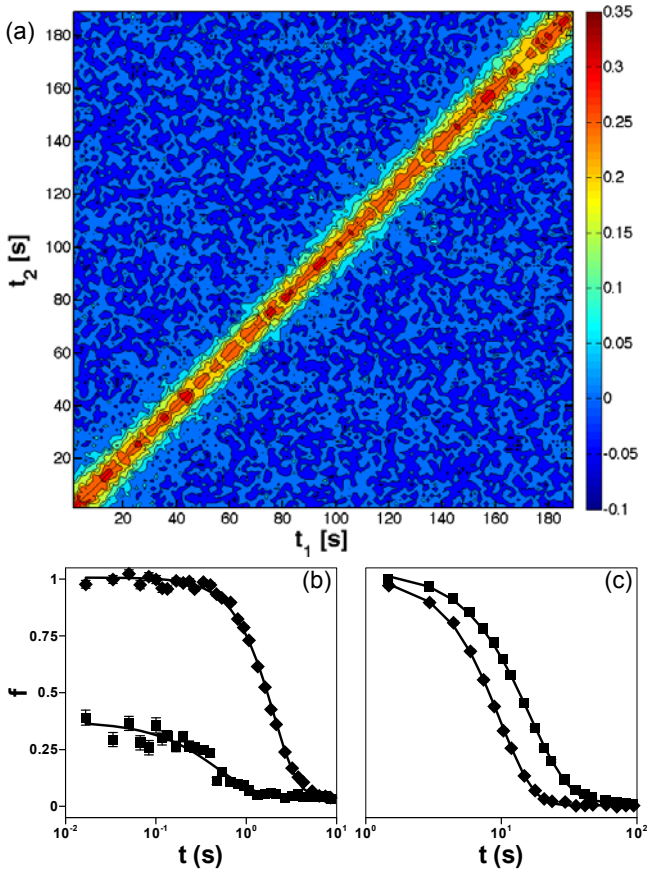

Figure 2| Temporal evolution of the scattering intensities. (a) A contour map of the two–time correlation function G for the d = 10 nm, ϕ = 0.35 suspension at q = 0.568 nm^{-1}. (b), (c) Dynamic structure factor $f(q,t)$ for d = 10 nm particle suspensions with (b) ϕ = 0.19 (squares), 0.27 (diamonds), (c) 0.30 (squares) and 0.35 (diamonds). Solid lines in (b) and (c) are compressed exponential fits.

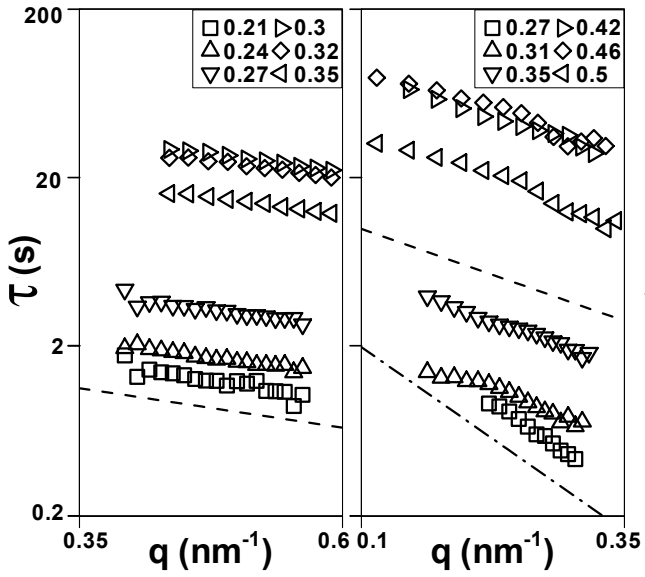

Figure 3| Wave vector dependence of relaxation time τ for d = 10 nm (left panel) and 24 nm (right panel). Dashed line denotes a $\tau \propto 1/q^2$, while the dash–dot line denotes $\tau \propto 1/q$ scaling.

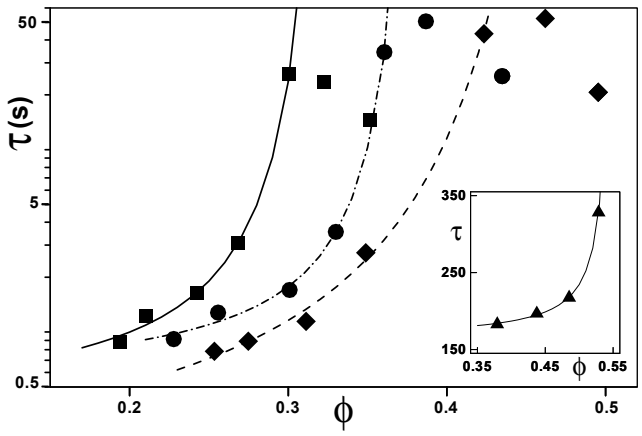

Figure 4| Particle loading dependence of the relaxation time τ for d = 10 nm (squares), 16 nm (circles), 24 nm (diamonds) and 40 nm (triangles, inset) suspensions. Lines indicate VFT fits. τ values reported at q = 0.49 nm^{-1}, 0.35 nm^{-1}, 0.19 $nm^{-1}$and 0.10 nm^{-1}, respectively.